WebLog Journal of Molecular and Cellular Biology

Review Article
Published: 10 Sep, 2026

Theoretical Investigation on NiF_2/Picolinic Acid-Catalyzed Chemoselective Coupling−Cyclization of 2-Iodobenzamide and Malonate to Furnish Homophthalimide

*Nan Lu**

College of Chemistry and Material Science, Shandong Agricultural University, Taian 271018, P. R. China

Abstract

The first theoretical investigation on NiF_2/picolinic acid-catalyzed chemoselective cou-pling–cyclization of 2-iodobenzamide and malonate was provided by our DFT calculation. First in Ni(I)/Ni(III) catalytic cycle, NiF_2 and PicA are converted to $L_2Ni(II)$ complex together with leaving of first HF molecule. Then malonate anion is generated from dimethyl malonate after removal of second HF molecule. The deprotona-tion of malonate gives enolate as single-electron reductant furnishing Ni(I) catalyst in concert modes. Next Ni(I) complex is coordinated with 2-iodobenzamide and undergoes oxidative addition providing aryl–Ni(III) intermediate. Subsequently, *via* trans-metalation with malonate anion replacing iodine, another Ni(III) species is produced bearing aryl and malonyl ligands. Reductive elimination delivered ortho-acylated benzamide intermediate and regenerated Ni(I) catalyst. Finally, homophthalimide product is yielded via intramolecular nucleophilic acyl substitution. That is base-promoted cyclization followed by methanol elimination which is also determined to be rate-limiting.

Keywords: NiF_2; Picolinic Acid; Cyclization; Benzamide; Homophthalimide

Introduction

Among cross-coupling process for construction of carbon framework, C–C bond formation catalyzed by Nickel has emerged as powerful strategy in synthetic chemistry [1, 2]. The reactivity complements other transition metals owing to versatility and cost advantage of nickel. However, many nickel-catalyzed annulations require external reductants. For example, direct C–H activation developed in benzamide-derived annulation. Kumon reported Cobalt-catalyzed C–H activation/annulation of benzamides with fluorine-containing alkynes [3]. Li discovered metal photo redox-catalyzed C–H activation in regio-selective annulation of allenes [4]. Zhang explored selective annulation of benzamides with internal alkynes catalyzed by an electron-deficient rhodium [5]. Rana obtained concise synthesis of quinisocaine in primary benzamide as coordinating Directing Group (DG) for Ru(II)-catalyzed C–H annulation [6]. There is also cascade coupling-cyclization of preactivated aryl halides such as axial-to-axial chirality transfer strategy for atroposelective construction of C–N axial chirality [7] and regio-divergent synthesis of methyl ring-fused isoquinolinones in base-promoted isomerization of N-allyl amides [8]. The limitation of these methods is relying on coordinating DGs [9, 10].

Photocatalysts are commonly required in photochemical annulation. Gong researched Nickel-catalyzed thermal redox functionalization of C (sp3)–H bonds with carbon electrophiles [11]. Wang exploited photo electrochemical Ni-catalyzed cross-coupling of aryl bromides with amine [12] and carboacylation/silanoylation of alkenes with unactivated C/Si–H bonds [13]. Zhou summarized Iron–Nickel synergistic catalysis for C (sp3)-H and dehydroxymethylative acylation [14]. Then 1,3-dicarbonyl nucleophiles provide an alternative annulation strategy yet malonate-based variants still less explored. Only CuI-catalyzed coupling of 2-bromobenzamides with β-Keto ester were developed to assemble substituted homophthalimides [15]. Until chelate compounds of Nickel (II) with picolinic acid were discovered, efficient coupling-cyclization was promoted without external reductant [16]. Despite nickel's reactivity toward amide C–N bonds such as con-version of amides to esters, alkylation of amide derivatives and activation of C–N bonds using non-precious-metal catalysis [17-20], the reductant-free condition and halide discrimination are difficult to overcome.

In this context, a recent breakthrough was NiF_2/picolinic acid-catalyzed chemoselective coupling-

OPEN ACCESS

Correspondence:
Dr. Nan Lu, College of Chemistry and Material Science, Shandong Agricultural University, Taian 271018, P. R. China, E-mail: lun@sdau.edu.cn

Received Date: *02 Aug 2026*
Accepted Date: *08 Sep 2026*
Published Date: *10 Sep 2026*

Citation:
Nan Lu. Theoretical Investigation on NiF_2/Picolinic Acid-Catalyzed Chemoselective Coupling−Cyclization of 2-Iodobenzamide and Malonate to Furnish Homophthalimide. WebLog J Mol Cell Biol. wjmcb.2026.i1001. https://doi.org/10.5281/zenodo.22848045

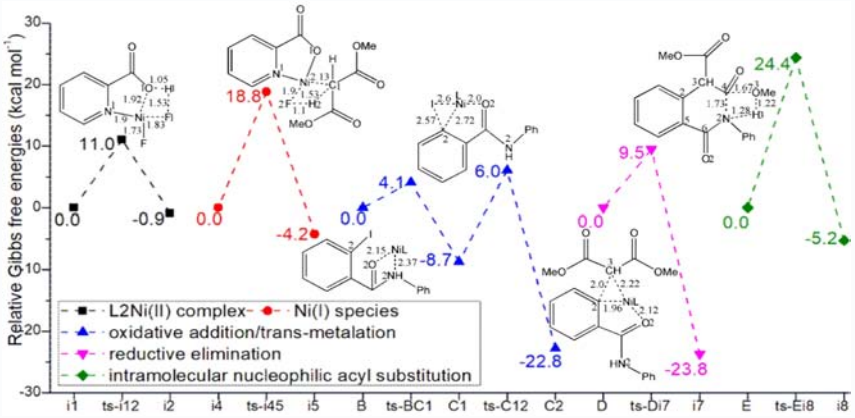

Figure 1: Relative Gibbs free energy profile in solvent phase starting from complex i1, i4, B, D, E (Bond lengths of opti-mized TSs in Å).

cyclization of 2-iodobenzamide and malonate of Tummatorn group [21]. Although 3-sulfonyl *α*-carboline was constructed, how NiF_2 performs superior enabling fluoride counterion in this transformation [22]? What's the concrete process of Ni(I)/Ni(III) catalytic cycle? How picolinic acid and NiF_2 are converted into chelating $L_2Ni(II)$ complex under basic condition? Single-electron oxidation has been exploited for transient radical cations as Brønsted acids in allylic C–H heteroarylation of enol silyl ethers as well as allylic C–H alkylation in photore-dox–Brønsted base hybrid catalysis [23, 24]. So, the step is significant involving deprotonation of malonate to enolate furnishing Ni(I) species. Since Ting has proposed oxidative addition of aryl halides to Ni(I)-bipyridine complex [25], here how the oxidative addition to 2-iodobenzamide provided aryl–Ni(III) intermediate?

Computational Details

Structures were optimized at M06-2X/6-31G(d) level with GAUSSIAN09 [26]. Among various DFT methods [27], M06-2X functional has smaller deviation between experimental and calculated value than B3LYP hybrid functional [28, 29]. With 6-31G(d) basis set, it can provide best compromise between time consumption and energy accuracy. It was also found to give accurate results for stepwise (2+2) cycloaddition, enantioselective (4+3) and Diels-Alder reaction [30, 31]. Together with good performance on noncovalent interaction, it is suitable for this system [32-34]. To obtain Zero-Point Vibrational Energy (ZPVE), harmonic frequency calculations were carried out at M06-2X/6-31G(d) level gaining thermodynamic corrections at 373 K and 1 atm in Tetrahydrofuran (THF). At M06-2X/6-311++G(d,p) level, the solvation-corrected free energies were obtained using Integral Equation Formalism Polarizable Continuum Model (IEFPCM) [35-39] on M06-2X/6-31G(d)-optimized geometries. NBO procedure was performed with Natural bond orbital (NBO3.1) obtaining lone pair and bond to characterize bonding orbital interaction and electronic properties [40-42]. Using Multiwfn_3.7_dev package [43].

Results and Discussion

The mechanism was explored for NiF_2/picolinic acid-catalyzed chemoselective coupling-cyclization of 2-iodobenzamide 1 and malonate 2 leading to homophthalimide 3 (Scheme 1). As illustrated by Scheme 2, as initial step of proposed Ni(I)/Ni(III) catalytic cycle, NiF_2 and Picolinic Acid (PicA) are converted into $L_2Ni(II)$ complex under basic condition together with leaving of one HF molecule. Then malonate anion is generated from dimethyl malonate 2 after removal of a second HF molecule. In this step, deprotonation of malonate gives an enolate that could act as single-electron reductant furnishing Ni(I) species A in concert modes. Next via coordination of A with 2-iodobenzamide 1, complex B is obtained which undergoes oxidative addition providing aryl-Ni(III) intermediate C through two steps. Subsequently, Ni(III) species D is produced *via* trans-metalation of C with another malonate anion replacing iodine. Therefore, D bears both aryl and malonyl ligands. Reductive elimination from D delivered ortho-acylated benzamide intermediate E and regenerated A. Finally, from E, intramolecular nucleophilic acyl substitution that is base-promoted cyclization followed by methanol elimination yielding homophthalimide product 3. Figure 1 listed schematic structures of optimized TSs in Scheme 2. Table 1 gave activation energy for all steps.

$L_2Ni(II)$ complex/Ni(I) species

In initial step of proposed Ni(I)/Ni(III) catalytic cycle, the first complex i1 is formed between NiF2 and PicA as starting point of step 1 (black dash line of Figure 1). Under basic condition, PicA was deprotonated *via* ts-i12 with the activation energy of 11.0 kcal mol^{-1} exothermic slightly by -0.9 kcal mol^{-1} resulting in i2. The transition vector corresponds to breaking of O1···H1, Ni···F1 and concerted bonding of H1···F1, Ni···O1 (1.05, 1.83, 1.53, 1.92 Å) (Figure S1a). After the leaving of one HF molecule, a $L_2Ni(II)$ complex denoted as i3 is obtained with two formal Ni-N1 and Ni-O1 coordinated bond.

Binding additional dimethyl malonate 2, i3 turns to be i4 as new starting point of step 2 (red dash line of Figure 1). In this step, deprotonation of malonate takes place *via* ts-i45 with increased activation energy of 18.8 kcal mol^{-1} exothermic by -4.2 kcal mol^{-1} forming i5. The transition vector includes stretching of Ni···F2, C1···H2 and concerted approaching of H2···F2, Ni···C1 (1.9, 1.53, 1.1, 2.13 Å) (Figure S1b). After removal of a second HF molecule, the enolate of 2 is given with negative charge located on C1 readily coordinated to Ni. Thus, without HF, i6 is generated involving a third coordinated bond Ni-C1, which could furnish Ni(I) complex A and malonate anion (2-H) acting as single-electron reductant in following process.

Oxidative addition/trans-metalation/reductive elimination/ intramolecular nucleophilic acyl substitution

Next the coordination of A and 2-iodobenzamide 1 with typical Ni-N2 makes complex B as new starting point of next two steps (blue dash line of Figure 1). Via ts-BC1 in step 3, B undergoes

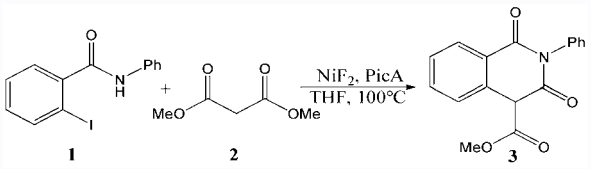

Scheme 1: NiF_2/picolinic acid-catalyzed chemoselective coupling-cyclization of 2-iodobenzamide 1 and malonate 2 leading to homophthalimide 3.

oxidative addition, the activation energy is decreased to 4.1 kcal mol^{-1} exothermic by -8.7 kcal mol^{-1} providing C1. The transition vector suggests coordination shifting from Ni···N2 to Ni···O2 (2.37, 2.15 Å). Subsequently from C1 via ts-C12 in step 4, the coordinated site of Ni moves to C2 of benzene ring still with weakened Ni-O2. The activation energy is 14.7 kcal mol^{-1} exothermic by -22.8 kcal mol^{-1} affording C2. Seen from the transition vector, the atomic motion is about closing of Ni···C2, Ni···I and resultant breaking down of C2···I (2.72, 2.6, 2.57 Å). Obviously, the aryl-Ni(III) intermediate C2 is rather stable with typical single bond Ni-C2 and Ni-I.

Through trans-metalation, the coordinated iodine I is replaced by malonate anion 2-H, C2 turns to be Ni(III) species D bearing aryl and malonyl ligands as new starting point of step 5 (magenta dash line of Figure 1). Then reductive elimination proceeds via ts-Di7 with decreased activation energy of 9.5 kcal mol^{-1} continuously exothermic by -23.8 kcal mol^{-1} delivering i7. The transition vector is about cleavage of Ni···C2, Ni···C3 and simultaneous linkage of C2···C3 (1.96, 2.22, 2.0 Å) (Figure S1c). When the typical C2-C3 single bond is formed, the Ni(I) catalyst A is also regenerated in i7.

After removal of recovered A, the ortho-acylated benzamide intermediate E is produced as new starting point of step 6 (olive dash line of Figure 1). From E, the intramolecular nucleophilic acyl substitution takes place *via* ts-Ei8 with activation energy of 24.4 kcal mol^{-1} exothermic by -5.2 kcal mol^{-1} affording i8. The transition vector reveals a complicated concert process that is base-promoted cyclization followed by methanol elimination. This includes C4···O3, N2···H3 breaking down and N2···C4, O3···H3 bonding (1.67, 1.28, 1.73, 1.22 Å) (Figure S1d). The formation of N2-C4 single bond completes

Table 1: The activation energy (in kcal mol^{-1}) of all reactions in gas and solvent.

TS	$\Delta G^{\neq}_{gas}$	$\Delta G^{\neq}_{sol}$
ts-i12	6.62	11.02
ts-i45	16.95	18.81
ts-BC1	5.83	4.10
ts-C12	14.62	14.70
ts-Di7	6.86	9.48
ts-Ei8	28.79	24.38

novel stable six-membered ring. The methanol molecule is furnished through O3-H3 afterwards. Finally, the homophthalimide product 3 is yielded after leaving of methanol. Comparatively, the nucleophilic acyl substitution of step 6 is determined to be rate-limiting for NiF_2/picolinic acid-catalyzed chemoselective coupling-cyclization of 2-iodobenzamide and malonate leading to homophthalimide.

Conclusions

In summary, the first theoretical investigation was provided by our DFT calculation on NiF_2/picolinic acid-catalyzed chemoselective coupling-cyclization of 2-iodobenzamide and malonate. First, NiF_2 and PicA are converted to $L_2Ni(II)$ complex together with leaving of one HF molecule as initial step of Ni(I)/Ni(III) catalytic cycle. Then malonate anion is generated from dimethyl malonate after removal of second HF molecule. The deprotonation of malonate gives enolate as single-electron reductant furnishing Ni(I) species catalyst in concert modes. Next the Ni(I) complex is coordinated with 2-iodobenzamide and undergoes oxidative addition providing aryl-Ni(III) intermediate through two steps.

Subsequently, *via* trans-metalation with malonate anion replacing iodine, another Ni(III) species is produced bearing aryl and malonyl ligands. Reductive elimination delivered ortho-acylated benzamide intermediate and regenerated Ni(I) catalyst. Finally, homophthalimide product is yielded *via* intramolecular nucleophilic acyl substitution. That is base-promoted cyclization followed by methanol elimination which is determined to be rate-limiting for the whole process.

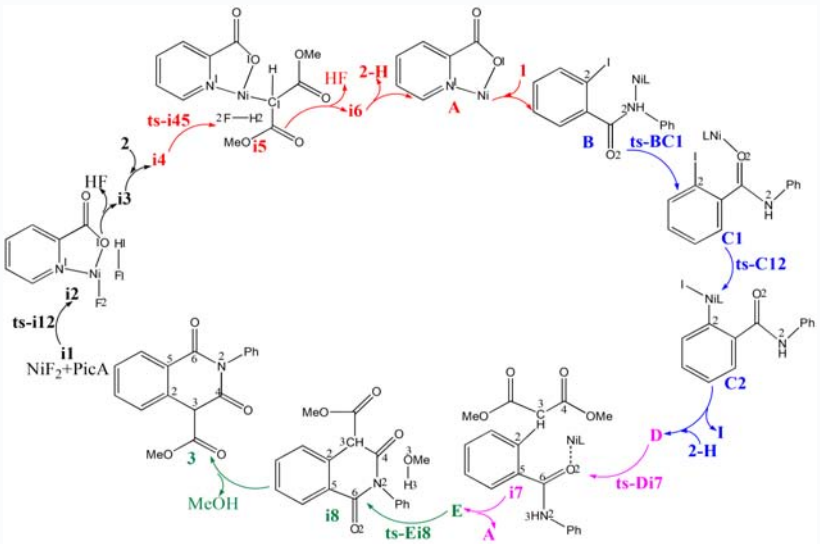

Scheme 2: Proposed reaction mechanism of NiF_2/picolinic acid-catalyzed chemoselective coupling-cyclization of 1 and 2 leading to 3. TS is named according to the two intermediates it connects.

Electronic Supplementary Material

Supplementary data available: [Computation information and cartesian coordinates of stationary points; Calculated relative energies for the ZPE-corrected Gibbs free energies (ΔG_{gas}), and Gibbs free energies (ΔG_{sol}) for all species in solution phase at 373 K.]

Author Contributions

Conceptualization: Nan Lu; Methodology, Nan Lu; Software, Nan Lu; Validation, Nan Lu; Formal Analysis, Nan Lu; Investigation, Nan Lu; Resources, Nan Lu; Data Curation, Nan Lu; Writing-Original Draft Preparation, Nan Lu; Writing-Review & Editing, Nan Lu; Visualization, Nan Lu; Supervision, Nan Lu; Project Administration, Nan Lu. All authors have read and agreed to the published version of the manuscript.

Funding

This work was supported by Key Laboratory of Agricultural Film Application of Ministry of Agriculture and Rural Affairs, P.R. China.

Conflict of Interest

The authors declare no conflict of interest.

References

1. Tsymbal AV, Bizzini LD, MacMillan DW. Nickel catalysis via SH2 homolytic substitution: the double decarboxylative cross-coupling of aliphatic acids. J Am Chem Soc. 2022; 144: 21278-21286.
2. Hsu CM, Lin HB, Hou XZ, Tapales RVPP, Shih CK, Miñoza S, et al. Azetidines with all-carbon quaternary centers: merging relay catalysis with strain release functionalization. J Am Chem Soc. 2023; 145: 19049-19059.
3. Kumon T, Wu J, Shimada M, Yamada S, Agou T, Fukumoto H, et al. Cobalt-catalyzed C–H activation/annulation of benzamides with fluorine-containing alkynes: A route to 3-and 4-fluoroalkylated isoquinolinones. J Org Chem. 2021: 86: 5183-5196.
4. Li T, Li J, Zhu Z, Chen Y, Li X, Yang Q, et al. Metallaphoto-redox-catalyzed C–H activation: regio-selective annulation of allenes with benzamide. Org Chem Front. 2021; 8: 928-935.
5. Zhang P, Chang W, Jiao H, Kang Y, Zhao W, Cui P, et al. Selective annulation of benzamides with internal alkynes catalyzed by an electron-deficient rhodium catalyst. Chin Chem Lett. 2021; 32: 1717-1720.
6. Rana T, Pawar AB. Primary Benzamide as a Weakly Coordinating Directing Group for Ru (II)-Catalyzed Redox-Neutral C–H Annulation: Concise Synthesis of Quinisocaine. J Org Chem. 2025; 90: 15271-15284.
7. Liu ZS, Xie PP, Hua Y, Wu C, Ma Y, Chen J, et al. An axial-to-axial chirality transfer strategy for atroposelective construction of C–N axial chirality. Chem. 2021; 7: 1917-1932.
8. Chen LY, Tang RS, Wu YC, Lai CH, Chuang TH. Regiodivergent Synthesis of Methylene and Methyl Ring-Fused Isoquinolinones: Base-Promoted Isomerization of N-Allyl Amides. J Org Chem. 2022; 87: 5925-5937.
9. Boos P, Pandit NK, Dana S, von Münchow T, Hashidoko A, Haberstock L, et al. Multiple Atropo Selectivity by κ_2-N, O-Oxazoline Urea Ligands in Cobaltaelec-tro-Catalyzed C–H Activations: Decoding Selectivity with Data Science Integration. Chem Eur. 2025; 3: e202500071.
10. Xu MY, Wang C, Jiang WT, Xiao B. Synthesis and Application of Heterocyclic Germatranes via Rhodium-Catalyzed Directed C– H Activation/Annulation with Alkynyl Germatranes and Palladi-um-Catalyzed Cross-Coupling. Adv Synth Catal. 2020; 362: 1706-1711.
11. Gong Y, Su L, Zhu Z, Ye Y, Gong H. Nickel-catalyzed thermal redox functionalization of C (sp3)– H bonds with carbon electrophiles. Angew Chem Int Ed Engl. 2022; 61: e202201662.
12. Wang J, Li S, Yang C, Gao H, Zuo L, Guo Z, et al. Photoelectro-chemical Ni-catalyzed cross-coupling of aryl bromides with amine at ultra-low potential. Nat Commun. 2024; 15: 6907.
13. Wang L, Huo X, He X, Ackermann L, Wang D. Photoelectrochemical nickel-catalyzed carboacyla-tion/silanoylation of alkenes with unactivated C/Si–H bonds. Green Chem. 2024; 26: 8315-8322.
14. Zhou X, Zhong PF, Li Z, Hu P, Tu J, Yang C, et al. Photoelectrochemical Iron–Nickel Synergistic Catalysis for C (sp3)-H and Dehydroxymethylative Acylation. Org Lett. 2025; 27: 6995-7000.
15. Wang H, Gao K, Jiang Y, Ma D. Assembly of substituted homophthalimides via CuI-catalyzed cou-pling of 2-bromobenzamides with β-Keto ester. Heterocycles. 2009; 79: 695-702.
16. Green, R. Chelate Compounds of Nickel (II) with Picolinic Acid. J Am Chem Soc. 1957; 79: 5608-5611.
17. Hie L, Nathel NF, Shah TK, Baker EL, Hong X, Yang YF, et al. Conversion of amides to esters by the nickel-catalysed activation of amide C–N bonds. Nature. 2015; 524: 79-83.
18. Simmons BJ, Weires NA, Dander JE, Garg NK. Nickel-catalyzed alkylation of amide derivatives. ACS Catal. 2016; 6: 3176-3179.
19. Dander JE, Garg NK. Breaking amides using nickel catalysis. ACS Catal. 2017; 7: 1413-1423.
20. Boit TB, Bulger AS, Dander JE, Garg NK. Activation of C–O and C–N bonds using non-precious-metal catalysis. ACS Catal. 2020; 10: 12109-12126.
21. Tanomsiri G, Takaoka J, Tummatorn J, Thongsornkleeb C, Ruchirawat S. Reductant-Free NiF 2 /Picolinic Acid-Catalyzed Coupling–Cyclization of 2 Iodobenzamides with Malonates. J Org Chem. 2026; 91(26): 8868-8880.
22. Ackerman LK, Lovell MM, Weix DJ. Multimetallic catalysed cross-coupling of aryl bromides with aryl triflates. Nature. 2015; 524: 454-457.
23. Ohmatsu K, Nakashima T, Sato M, Ooi T. Direct allylic C–H alkylation of enol silyl ethers enabled by photoredox–Brønsted base hybrid catalysis. Nat. Commun. 2019; 10: 2706.
24. Nakashima T, Fujimori H, Ohmatsu K, Ooi T. Exploiting transient radical cations as Brønsted acids for allylic C–H heteroarylation of enol silyl ethers. Chem Eur J. 2021; 27: 9253-9256.
25. Ting SI, Williams WL, Doyle AG. Oxidative addition of aryl halides to a Ni (I)-bipyridine complex. J Am Chem Soc. 2022; 144: 5575-5582.
26. Frisch MJ, Trucks GW, Schlegel HB, Frisch MJ, Trucks GW, Schlegel J, et al. Gaussian 09 (Revision B.01). Gaussian Inc. 2010.
27. Stephens PJ, Devlin FJ, Chabalowski CF, Frisch MJ. Ab initio Calculation of Vibrational Absorp-tion and Circular Dichroism Spectra Using Density Functional Force Fields. J Phys Chem. 1994; 98: 11623-11627.
28. Becke AD. Density-functional thermochemistry. IV. A new dynamical correlation functional and im-plications for exact-exchange mixing. J Chem Phys. 1996; 104: 1040-1046.
29. Lee CT, Yang WT, Parr RG. Development of the Colle-Salvetti correlation-energy formula into a functional of the electron density. Phys Rev B Condens Matter. 1988; 37: 785-789.
30. Li X, Kong X, Yang S, Meng M, Zhan X, Zeng M, et al. Bifunctional Thiourea-Catalyzed Asym-metric Inverse-Electron-Demand Diels-Alder Reaction of Allyl Ketones and Vinyl 1,2-Diketones via Dienolate Intermediate. Org Lett. 2019; 21: 1979-1983.
31. Krenske EH, Houk KN, Harmata M. Computational Analysis of the Stereochemical Outcome in the Imidazolidinone-Catalyzed Enantioselective (4 + 3)-Cycloaddition Reaction. J Org Chem. 2015; 80: 744-750.
32. Lv H, Han F, Wang N, Lu N, Song Z, Zhang J, et al. Ionic Liquid Catalyzed

C-C Bond Formation for the Synthesis of Polysubstituted Olefins. Eur J Org Chem. 2022; 2022(45): e202201222.

33. Zhuang H, Lu N, Ji N, Han F, Miao C. Bu4NHSO4-Catalyzed Direct N-Allylation of Pyrazole and its Derivatives with Allylic Alcohols in Water: A Metal-free, Recyclable and Sustainable System. Adv Synth Catal. 2021; 363: 5461-5472.

34. Lu N, Liang H, Qian P, Lan X, Miao C. Theoretical investigation on the mechanism and enantiose-lectivity of organocatalytic asymmetric Povarov reactions of anilines and aldehydes. Int J Quantum Chem. 2020; 120: e26574.

35. Tapia O. Solvent effect theories: Quantum and classical formalisms and their applications in chemistry and biochemistry. J Math Chem. 1992; 10: 139-181.

36. Tomasi J, Persico M. Molecular Interactions in Solution: An Overview of Methods Based on Continu-ous Distributions of the Solvent. Chem Rev. 1994; 94: 2027-2094.

37. Simkin BY, Sheikhet I. Quantum Chemical and Statistical Theory of Solutions—A Computational Approach. Ellis Horwood. 1995.

38. Tomasi J, Mennucci B, Cammi R. Quantum Mechanical Continuum Solvation Models. Chem Rev. 2005; 105: 2999-3093.

39. Marenich AV, Cramer CJ, Truhlar DG. Universal Solvation Model Based on Solute Electron Density and on a Continuum Model of the Solvent Defined by the Bulk Dielectric Constant and Atomic Sur-face Tensions. J Phys Chem B. 2009; 113: 6378-6396.

40. Reed AE, Weinstock RB, Weinhold F. Natural population analysis. J Chem Phys. 1985; 83: 735-746.

41. Reed AE, Curtiss LA, Weinhold F. Intermolecular interactions from a natural bond orbital do-nor-acceptor view point. Chem Rev. 1988; 88: 899-926.

42. Foresman JB, Frisch A. Exploring Chemistry with Electronic Structure Methods, 2nd ed., Gaussian Inc. 1996.

43. Lu T, Chen F. Multiwfn: A multifunctional wavefunction analyzer. J Comput Chem. 2012; 33: 580-592.